11th World Congress on Computational Mechanics (WCCM XI)
5th European Conference on Computational Mechanics (ECCM V)
6th European Conference on Computational Fluid Dynamics (ECFD VI)
E. Oñate, J. Oliver and A. Huerta(Eds)

COMPUTATIONAL AND EXPERIMENTAL INVESTIGATION OF THE ALL FRACTURE MODE SPECIMENS ON I/III AND II/III FRACTURE

SHI-FAN ZHU[1,*], YANG CAO[2], QING-FEN LI[3] AND LI ZHU[4]

College of Mechanical and Electrical Engineering, Harbin Engineering University
150001 Harbin, China
e-mail: [1]zhushifan@hrbeu.edu.cn, [2]caoyang@hrbeu.edu.cn, [3]liqingfen@hrbeu.edu.cn, [4]zhuli@hrbeu.edu.cn

Key Words: *Mixed mode fracture, Finite element analysis, Stress intensity factors.*

Abstract. In this paper, the fracture behavior in AFM specimen with a single edged crack under I+III and II+III loading conditions is investigated by both computational analysis and experimental investigations. The non-dimensional stress intensity factors (Y values) along the crack front were calculated by the virtual crack closure (VCC) method and commercial software ANSYS. The AFM specimens made by polymethyl methacrylate material were used for experimental investigations. Tests were performed in according with GB/T4161-2007 and carried out on an Instron 4505 testing machine under mixed mode I+III and II+III loading conditions. The complete fracture process was observed from crack initial break, unstable propagation to final fracture. Results show that the experimental findings were in agreement with the computational results.

1 INTRODUCTION

Fracture processes are in many cases of the three dimensional (3D) character in the real engineering structures. However, the prediction of the developing 3D fracture process is not well understood yet. In particular there is a shortage of experimental findings regarding general 3D and mixed-mode fracture to form a solid basis on which the desired understanding and the missing fracture criteria could be established [1]. The finite element method (FEM) has been used with great success in the computational fracture mechanics in the past several decades, and in recent years, several promising methods of modeling have been developed [2,3]. Although the investigation of 3D crack configurations has been a major task of fracture-mechanical research for a long time, the description of the crack deflection under general mixed-mode loading is still unsolved. Further investigations have to be performed in order to improve this situation.

In this paper, the fracture behavior in AFM specimen with a single edged crack under I+III and II+III loading conditions is investigated by both computational analysis and experimental investigations.

2 COMPUTATIONAL FRACTURE ANALYSIS

The AFM loading device and specimen designed by our research group based on Richard [4] are shown in Figure 1. Through the AFM loading device all single types of loading can be generated and furthermore arbitrary combinations of external tension, in-plane shear and out-of-plane shear loadings can be achieved. The AFM-specimen is a special type of single edge notched (SEN) specimen (Figure 1 b). The geometrical parameters of AFM-specimen, in Figure 1 c), are as follows: width W =27mm, thickness t =24.3mm, crack length a =0.5 W (straight crack front), H_1 =32.5mm, and H_2 =57.5mm. The material parameters are chosen as follows: Young's modulus $E = 2.1\times10^5$ N/mm^2 and Poisson's ratio ν =0.3. The specimen is subject to a static loading of F =6561N.

When the load F is acting under the angles α and β with respect to the local crack or notch tip coordinate system the components of F can be expressed in Eq.1：

$$\left.\begin{aligned} N &= F_y = F\cos\alpha \\ Q &= F_x = F\sin\alpha\cos\beta \\ T &= F_z = F\sin\alpha\sin\beta \\ M_Q &= FH_2\sin\alpha\cos\beta \\ M_T &= FH_1\sin\alpha\sin\beta \end{aligned}\right\} \quad (1)$$

The 3D FE-model of the AFM-specimen is assembled of some standard 6- but predominantly of non-singular, standard 8-node volume elements. The total mesh consists of 14132 six- or eight-node SOLID45 elements with a total of 17626 nodes. A spider-web-like mesh around the crack front is employed near the crack front to capture detailed stress/strain variations and their singularity behavior. Considering the singular stress behavior at the crack front some mesh refinement is incorporated in the model adjacent to the crack front and with respect to the MVCCI-method the crack front is formed by a homogeneous mesh with elements of constant size ($0.1\times0.1\times0.1\text{mm}^3$ with $\Delta a = 0.1$mm and $\Delta a/a = 0.0074$).

The AFM specimen with a single edged crack under I+III（α=45°, β=90°） and II+III（α=90°,β=45°）loading conditions are shown respectively in Figure2.

3 EXPERIMENT AND DISCUSSION

The AFM specimens made by polymethyl methacrylate（PMMA）material were used for experimental investigations. The mechanical parameters of the PMMA material are shown in Table 1.Tests were performed in according with GB/T4161-2007 and carried out on an Instron 4505 testing machine under mixed mode I+III and II+III loading conditions (Figure3). The complete fracture process was observed from crack initial break, unstable propagation to final fracture.

Table 1 Mechanical parameters of test material PMMA

Elasticity modulus	Yield strength σ_s	Tensile strength σ_b	Poisson's ratio ν
3150MPa	47.5MPa	70.0MPa	0.36

4 RESULTS AND DISCUSSION

The non-dimensional stress intensity factors (Y values) along the crack front of 3D FE-model calculated by the virtual crack closure (VCC) method and commercial software

ANSYS for mixed mode I+III and II+III loading are shown in Figure 4 and Figure 6 respectively. The effective Y_{eff}-values obtained by combination of both the Richard criteria and the present work are shown in Figure 5 and Figure 7 respectively.

From Figure 4, the Y_I and Y_{III} values are found to be nearly constant in the inner part of the specimen (-0.3< z/B <0.3), the Y_I -values decreased and the Y_{III} -values increased when adjacent to the free surface of the specimen. The behavior is related to Poisson's ratio. The Y_{II} -values increased along the crack front with the minim value at one corner (z/B=-0.5) and the maxim value at the other corner (z/B=+0.5).

Figure 5 shows that the effective Y_{eff}-values for mode I+III loading reach the maximum at the free surface of the specimen($z/B = \pm 0.5$). We may conclude that for mode I+III loading condition, the fracture will occur at two corners of the crack front firstly and simultaneously.

From Figure 6, it is found that the Y_I values are always zero, indicating that the stress of mode I may not be produced on II+III loading condition. The Y_{II} and Y_{III} values increased gradually for the most part of the crack front from one corner (z/B=-0.5) to the other corner (z/B=+0.5). It can also be seen that the Y_{II} and Y_{III} values achieved along the crack front are more complex since when the mode II and III loads are applied together on the specimen, the applied and induced modes are generated simultaneously. For $z/B \geq 0$, the Y_{II} and Y_{III} values are the results of the applied modes plus the induced ones, whereas, for z/B <0, they are the results of the applied modes offset the induced ones. Finally, the total Y_{II} and Y_{III} values are evaluated that they increase along the crack front with the minim value at one corner and the maxim value at the other corner. It can therefore be predicted that the fracture will occur initially at one corner on the crack front of the AFM-specimen.

Figure 7 shows that the effective Y_{eff}-values for mode II+III loading rapidly reach the maximum at the free surface of the specimen(z/B=+0.5). It can be concluded that for mode II+III loading condition, the fracture will occur firstly at one corner on the crack front of the AFM-specimen.

The fracture process was observed and the final fractured specimen for I+III and II+III loading test are shown in Figure 8 and 9 respectively. It is obvious that the fracture occur at two corners of the crack front firstly and simultaneously for I+III loading, and that the fracture occur initially at one corner on the crack front of the specimen for mode II+III loading condition. Results show that the experimental findings were in agreement with the computational results.

REFERENCES

[1] Buchholz, F.-G., Chergui, A. and Richard, H.A. Fracture analyses and experimental results of crack growth under general mixed mode loading conditions. *Engng. Frac. Mech*. (2004) Vol. 71: 455-468.

[2] Li, Q., Zhu, L., Zhu, S., Buchholz, F.-G. Fracture behavior in AFM-specimen with single crack under different loading conditions. *Structural Durability and Health Monitoring* (2010) Vol.6: 273-288,.

[3] Richard, H.A., Schramm, B. and Schirmeisen, N.H. Cracks on mixed mode loading - theories, experiments, simulations. *Int. J. Fatigue*, Article in press, 2013.

[4] Richard, H.A. and Kuna, M. Theoretical and experimental study of superimposed fracture modes I, II and III. *Engng. Frac. Mech*. (1990) Vol. 35: 949-960.

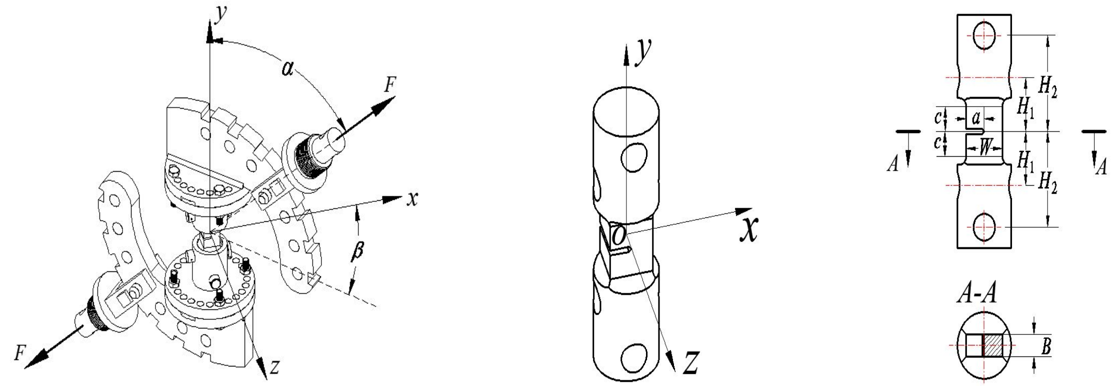

(a) AFM-specimen mounted in loading device (b) AFM-specimen (c) AFM-specimen size

Figure 1 AFM loading device and specimen

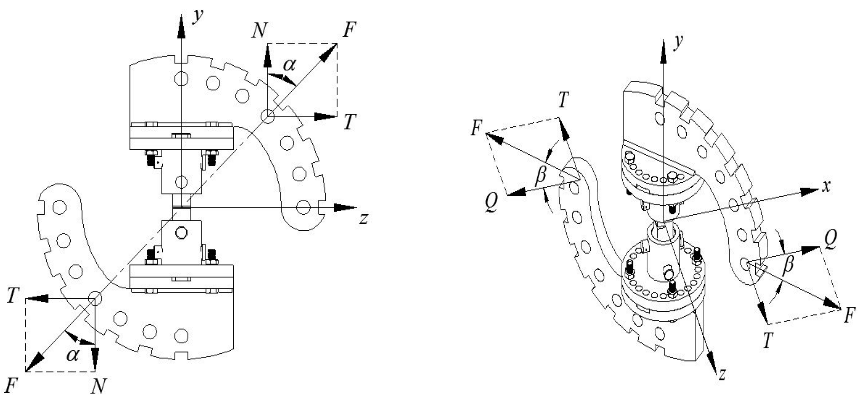

(a) I+III loading (b) II+III loading

Figure 2 Schematic diagram of mixed mode fracture test

(a) I+III loading (b) II+III loading

Figure 3 Experiment devices for mixed mode loading

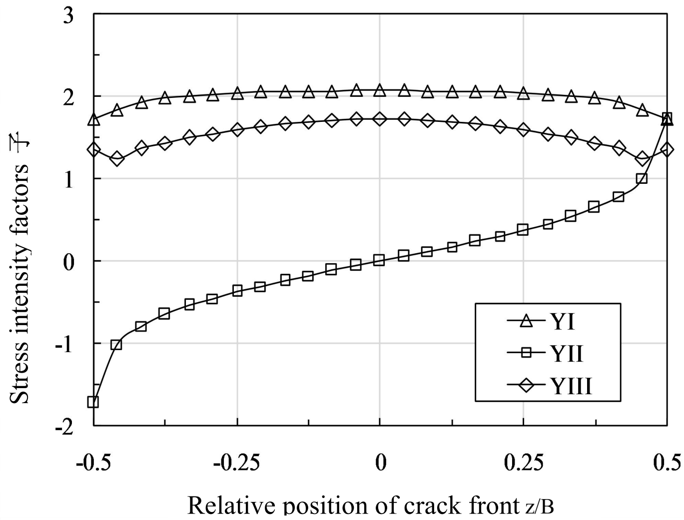

Figure 4 Y-value along the crack front of AFM model under mixed mode I+III loading

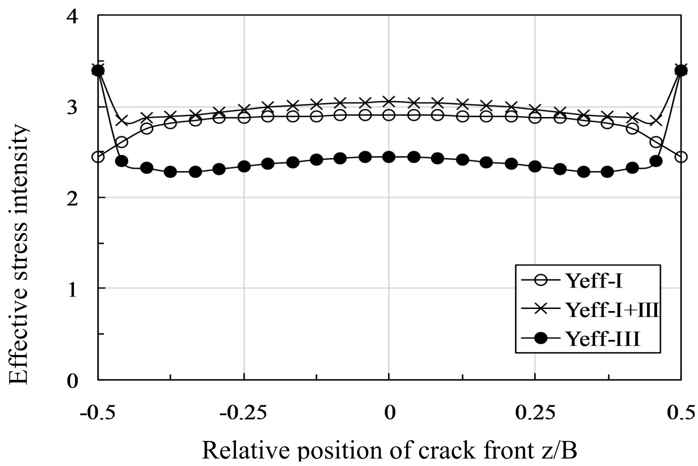

Figure 5 Y_{eff}-value along the crack front of AFM model under mixed mode I+III loading

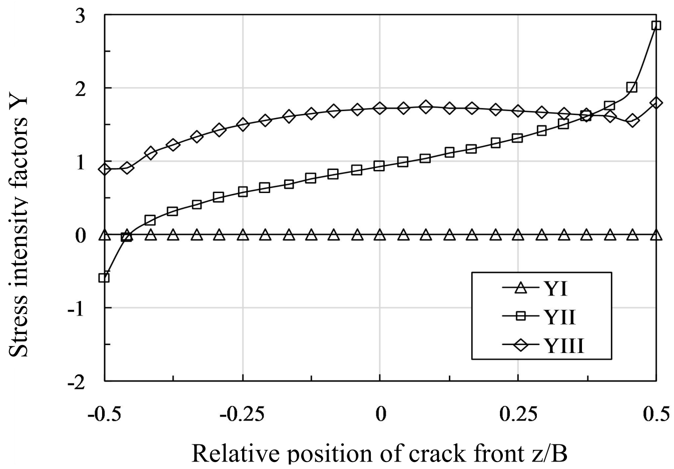

Figure 6 Y-value along the crack front of AFM model under mixed mode II +III loading

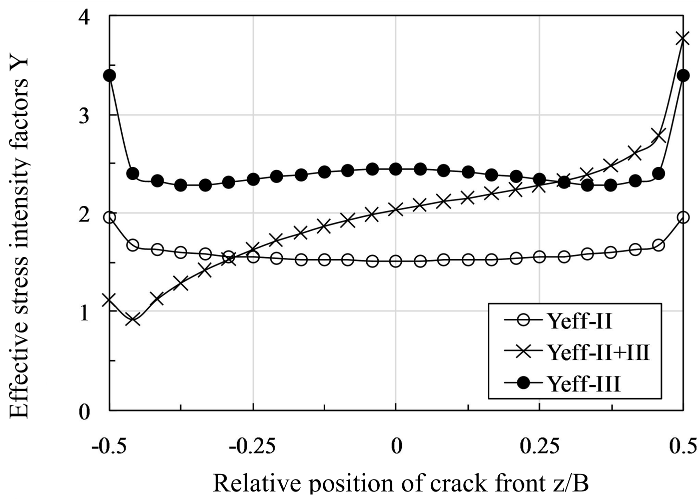

Figure 7 Y_{eff}-value along the crack front of AFM model under mixed mode II +III loading

(a) Oblique view (b) Back view

Figure 8 Final fractured specimen for I+III loading

(a) Left view (b) Back view (c) Oblique view

Figure 9 Final fractured specimen for II+III loading